JOURNAL OF BACTERIOLOGY, June 1996, p. 3641–3649 Vol. 178, No. 12
0021-9193/96/$04.00+0

Oxidative Stress Response and Its Role in Sensitivity to Isoniazid in Mycobacteria: Characterization and Inducibility of *ahpC* by Peroxides in *Mycobacterium smegmatis* and Lack of Expression in *M. aurum* and *M. tuberculosis*

S. DHANDAYUTHAPANI, Y. ZHANG, M. H. MUDD, AND V. DERETIC*

Department of Microbiology, University of Texas Health Science Center at San Antonio, San Antonio, Texas 78284-7758

Received 19 January 1996/Accepted 8 April 1996

***Mycobacterium tuberculosis* is a natural mutant with inactivated oxidative stress regulatory gene *oxyR*. This characteristic has been linked to the exquisite sensitivity of *M. tuberculosis* to isonicotinic acid hydrazide (INH). In the majority of mycobacteria tested, including *M. tuberculosis*, *oxyR* is divergently transcribed from *ahpC*, a gene encoding a homolog of the subunit of alkyl hydroperoxide reductase that carries out substrate peroxide reduction. Here we compared *ahpC* expression in *Mycobacterium smegmatis*, a mycobacterium less sensitive to INH, with that in two highly INH sensitive species, *M. tuberculosis* and *Mycobacterium aurum*. The *ahpC* gene of *M. smegmatis* was cloned and characterized, and the 5′ ends of *ahpC* mRNA were mapped by S1 nuclease protection analysis. *M. smegmatis* AhpC and eight other polypeptides were inducible by exposure to H_2O_2 or organic peroxides, as determined by metabolic labeling and Western blot (immunoblot) analysis. In contrast, *M. aurum* displayed differential induction of only one 18-kDa polypeptide when exposed to organic peroxides. AhpC could not be detected in this organism by immunological means. AhpC was also below detection levels in *M. tuberculosis* H37Rv. These observations are consistent with the interpretation that *ahpC* expression and INH sensitivity are inversely correlated in the mycobacterial species tested. In further support of this conclusion, the presence of plasmid-borne *ahpC* reduced *M. smegmatis* susceptibility to INH. Interestingly, mutations in the intergenic region between *oxyR* and *ahpC* were identified and increased *ahpC* expression observed in Δ*katG M. tuberculosis* and *Mycobacterium bovis* INH^r strains. We propose that mutations activating *ahpC* expression may contribute to the emergence of INH^r strains.**

In addition to its clinical significance as a front-line antituberculosis agent (37, 39, 42), isonicotinic acid hydrazide (isoniazid; INH) is becoming increasingly useful in dissecting the genetics and physiology of oxidative stress response in mycobacteria (8, 24, 41, 42). This more recent spin-off of a long history of extensive studies initially focused primarily on *Mycobacterium tuberculosis* sensitivity to INH is based on the apparent role that systems defending bacterial cells against reactive oxygen intermediates play in mycobacterial susceptibility to INH (13, 25, 41, 42). A correlation between INH resistance in *M. tuberculosis* and reduced activity of catalase-peroxidase, an enzyme which in other bacteria plays a role in detoxification of endogenously generated or exogenously supplied hydrogen peroxide (4, 10, 19), became apparent as soon as INH was introduced into clinical practice as a potent antituberculosis agent (20). In recent years, mutations in the gene for catalase-peroxidase, *katG*, have been described as a major mechanism contributing to the emergence of INH resistance in clinical isolates (13, 22, 41) and have been characterized in several series of isogenic INH^s and INH^r strains selected under laboratory conditions (25). However, not all INH^r strains have mutations in *katG* (13, 22) or in another locus, *inhA*, implicated in mycolic acid synthesis and believed to represent a target for INH action (2). Thus, while significant insights have been gained from these studies, additional work is needed to provide a comprehensive understanding of the mechanisms of resistance to INH in *M. tuberculosis*. Moreover, the reasons underlying the exquisite sensitivity of *M. tuberculosis* to INH, which is several orders of magnitude higher than that in most mycobacteria, remain to be clearly defined, although some recent progress has been made (2, 8).

We have recently expanded investigations of the oxidative stress response in *M. tuberculosis* (8, 9, 12) to genes besides *katG* with a twofold rationale: (i) it seemed possible that other members of the oxidative stress response, including regulatory factors, could participate in the processes related to INH susceptibility; and (ii) it appeared that a broader analysis of the oxidative stress response in *M. tuberculosis* might provide additional insights regarding its basic biology, including the capacity to survive in macrophages, an issue of importance for the host-pathogen interactions in tuberculosis (6). As one of the first findings resulting from such investigations, we have recently reported (8) that *M. tuberculosis* and other members of the *M. tuberculosis* complex are natural mutants with multiple lesions in *oxyR* (Fig. 1A). Similar observations have been made by others (28). In contrast to *M. tuberculosis*, a complete *oxyR* gene has been found in other mycobacteria studied (8, 28). This gene has been proposed to represent a functional equivalent of *oxyR*, the well-characterized central regulator of peroxide stress response in enteric bacteria (4, 35). This notion has been further reinforced (8, 28) by the linkage and arrangement of *oxyR* and *ahpC*, a gene encoding a close homolog of the alkyl hydroperoxide reductase subunit which carries out the reduction of substrate peroxides (16) and is a member of the *oxyR*-dependent peroxide-inducible branch of the oxidative stress response in enteric bacteria (4, 10, 39). Although *oxyR*

* Corresponding author. Current address: Department of Microbiology and Immunology, 5641 Medical Science Building II, University of Michigan Medical School, Ann Arbor, MI 48109-0620. Phone: (313) 763-1580. Fax: (313) 764-3562. Electronic mail address: Deretic @umich.edu.

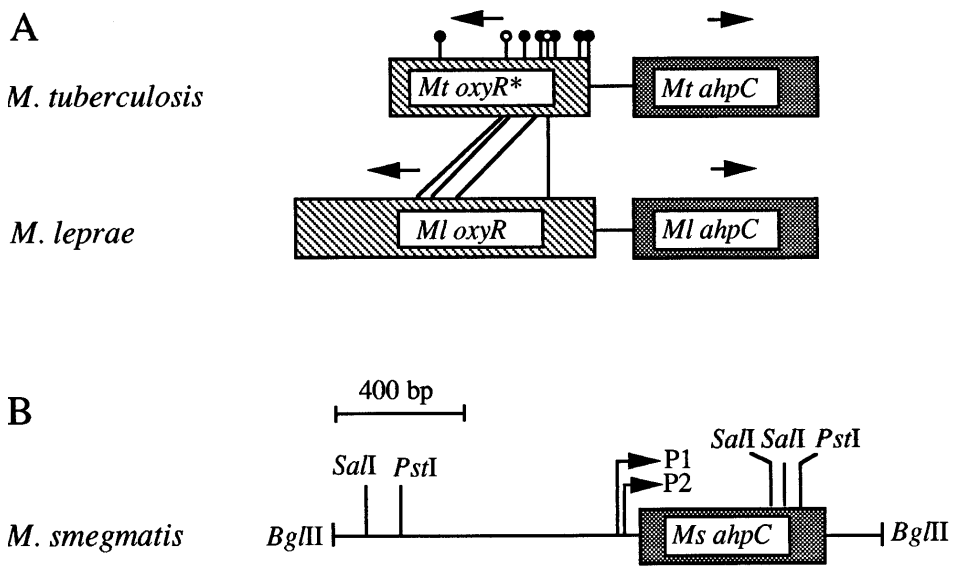

FIG. 1. Schematic representation of the genetic organization of the *ahpC* and *oxyR* genes in mycobacteria. (A) In the majority of mycobacterial species tested (8), *oxyR* and *ahpC* are tightly linked and divergently transcribed (overhead arrows), as exemplified by *M. leprae oxyR* and *ahpC*. The *oxyR* gene in *M. tuberculosis* (*Mt oxyR**; the asterisk indicates inactive gene) has multiple mutations: absence of a start codon, nonsense or frameshift lesions (filled balloons), and large deletions (open balloons). Lines connecting *M. tuberculosis oxyR* and *M. leprae oxyR* (*Ml oxyR*) denote the 29-bp and 372-bp deletions predicted in *M. tuberculosis* relative to *M. leprae* (8). (B) Chromosomal region (1.7-kb *Bgl*II fragment) with *M. smegmatis ahpC* (*Ms ahpC*). The complete sequence of this region (GenBank accession numbers U31978 and U43719) has been determined, and no *oxyR* could be identified upstream of *ahpC*. Bent arrows, two *ahpC* mRNA 5′ ends (P1 and P2).

and *ahpC* are not genetically linked in enteric bacteria, *oxyR* in *Escherichia coli* is juxtaposed to and divergently transcribed from *oxyS*, a gene that it regulates in addition to *ahpC*, *dps*, *gorA*, and *katG*, which are located elsewhere on the chromosome (35). This arrangement in enteric bacteria and the genetic organization (Fig. 1) in *Mycobacterium leprae* and the *M. tuberculosis* complex, with the divergently transcribed *oxyR* and *ahpC* separated by 105 to 121 bp, are typical of the LysR family of transcriptional regulators (26).

In addition to uncovering the multiple lesions in *M. tuberculosis oxyR*, we have also presented evidence that the loss of *oxyR* function in *M. tuberculosis* may be related to the processes causing high sensitivity of *M. tuberculosis* to INH (8). *M. tuberculosis* H37Rv, which is normally sensitive to 0.05 μg of INH per ml, becomes resistant to 5 μg of INH per ml when transformed with plasmids containing the *M. leprae oxyR-ahpC* region with intact *oxyR* (8). These findings support the notion that *oxyR* lesions in *M. tuberculosis* affect INH sensitivity, possibly by depriving this organism of physiological induction of *ahpC*. However, effects of the lesions in *oxyR* on activities of other genes, potentially controlled by this regulator, cannot be excluded in this context. In this work, we characterized the *ahpC* gene and examined its expression in *Mycobacterium smegmatis*, a species that is relatively insensitive to INH. We also compared the levels of *ahpC* expression in *M. smegmatis* and the two exquisitely INH sensitive species, *M. tuberculosis* and *Mycobacterium aurum*. Because of its intrinsic sensitivity to INH (14), the rapidly growing *M. aurum* can replace the slowly growing *M. tuberculosis* in bioassays used to determine INH blood levels for clinical or compliance monitoring purposes (18). We show that in *M. smegmatis*, AhpC is detectable under standard growth conditions and is additionally inducible upon

TABLE 1. Bacterial strains and plasmids used

Strain or plasmid	Relevant properties[a]	Source or reference
Mycobacteria		
M. aurum ATCC 23366	Species type strain; INH^s (MIC < 1 μg/ml)	ATCC[b]
M. bovis ATCC 35735	*M. bovis* BCG Montreal INH^s $katG^+$ *ahpCp* wt	ATCC
M. bovis ATCC 35747	INH^r derivative of *M. bovis* BCG Montreal; Δ*katG* (partial), *oxyR-ahpCp*(C→T)$_{-54}$	ATCC; 25
M. smegmatis mc^2155		30
M. tuberculosis H37Rv	INH^s $katG^+$ *ahpCp* wt	ATCC
M. tuberculosis 24	Clinical INH^r strain; Δ*katG*; *oxyR-ahpCp*(C→T)$_{-54}$	41
M. tuberculosis B1453	Clinical INH^r strain; Δ*katG*; *oxyR-ahpCp*(T→A)$_{-76}$ *oxyR-ahpCp*(G→A)$_{-88}$	41
Plasmids		
pDP81	*ahpC* (*M. smegmatis*) in pBlueskript(SK)	This work
p*MsahpC*	*ahpC* (*M. smegmatis*) in pMV206 (*oriM oriE* Km^r)	This work
pVDtb#3	*oxyR-ahpC* (*M. tuberculosis*); 5.5-kb *Bam*HI insert from cosmid T183 in pUC12	8
p*MtahpC*	*ahpC* (*M. tuberculosis*) in pSMT3 (*oriM* Hyg^r)	This work
p*Mthis*$_{10}$*-ahpC*	*his*$_{10}$*-ahpC* (*M. tuberculosis*) in pET-16b (T7 expression vector)	This work

[a] *oxyR-ahpCp* (*X*→*Y*)$_z$, *oxyR-ahpC* intergenic region alleles; nucleotide substitutions (*X*→*Y*) are given relative to *M. tuberculosis* H37Rv coordinates with the negative numbering (*z* in subscript) reflecting position from the *ahpC* start codon. wt, wild type.
[b] ATCC, American Type Culture Collection.

exposure to peroxides, in sharp contrast to the low or undetectable levels of AhpC in *M. tuberculosis* and *M. aurum*. At the genetic level, we present the molecular characterization of *ahpC* and its promoter, demonstrate that elevated expression of *ahpC* can increase the threshold for inhibition of *M. smegmatis* growth by INH, and report point mutations within the *oxyR-ahpC* intergenic region in *M. tuberculosis.*

MATERIALS AND METHODS

Bacterial strains, plasmids, media, and growth conditions. Bacterial strains and plasmids are described in Table 1. *M. aurum* type strain ATCC 23366 was obtained from the American Type Culture Collection; the MIC of INH for this strain was <0.625 μg/ml in different media. Similar sensitivity of this strain (<1 μg of INH per ml) has been observed by Lacave (17a). *M. bovis* ATCC 35747 is an INH^r derivative of *M. bovis* BCG Montreal, characterized by Rouse and Morris (25) as a *katG* null mutant (507-bp deletion removing the 5′ end of *katG*). *M. tuberculosis* 24 and B1453 are the two Δ*katG* INH^r clinical strains described in the initial report on the correlation between *katG* mutations and INH resistance (41). Plasmid p*Mthis$_{10}$-ahpC* was constructed by modifying the 5′ end of *M. tuberculosis ahpC*, using PCR with primers TBahpFW (5′ ATGAGGAGA CATATGCCACTGCTA3′; *Nde*I site underlined) and TBahpRV (5′CCCGGC CAACCGGATCCCGGTTAG3′; *Bam*HI site underlined) and pVDtb#3 the as template. The PCR product was cloned in pCRII (Invitrogen), excised as *Nde*I and *Bam*HI, and inserted into *Nde*I-*Bam*HI-digested pET16b to generate p*Mthis$_{10}$-ahpC*. All mycobacteria were grown in Middlebrook 7H9 medium or on 7H10 plates (Difco Laboratories) supplemented with 0.05% Tween 80 and ADC enrichment for *M. smegmatis* and *M. aurum* or OADC enrichment for *M. tuberculosis*. All manipulations of live *M. tuberculosis* organisms were carried out under biosafety level 3 conditions. *M. tuberculosis* was inactivated by heating at 80°C for 1 h. *E. coli* was grown on LB. All incubations were at 37°C except for *M. aurum*, which was grown at 30°C. Antibiotics were supplemented when necessary as follows: 25 μg of kanamycin per ml for *E. coli* and *M. smegmatis*, 50 μg of hygromycin per ml for *E. coli* and *M. tuberculosis*, and 50 μg of ampicillin per ml for *E. coli.*

Recombinant DNA techniques, genetic methods, and sequence analysis. Chromosomal isolation, Southern blotting, *E. coli* transformation, cloning procedures, and nucleotide sequence determination were based on standard methods or previously published modifications (1, 8, 15). Electroporation of *M. smegmatis* and *M. tuberculosis* was carried out as previously described (15).

Cloning of *M. smegmatis ahpC*. The hybridization probe used to detect and clone *M. smegmatis ahpC* was obtained by PCR using the previously described primers Ahp1P and OxyR5 (8) and plasmid pVDtb#3, carrying a 5.5-kb *Bam*HI insert with *M. tuberculosis oxyR* and *ahpC*. To isolate *ahpC* from *M. smegmatis*, a partial library of *M. smegmatis* genomic DNA was made by eluting *Bgl*II-digested DNA (1.5- to 2-kb region) from an agarose gel and cloning it into the *Bam*HI site of pBluescript(SK). Transformants were grown in pools of 12 per plate, and bacterial outgrowths were scraped and subjected to plasmid extraction and Southern blot analysis using the probe used to detect *ahpC* on genomic blots. After screening of 18 pools of 12 recombinants (a total of 216 independent clones), a positive pool was identified and subjected to another cycle of hybridization analysis of individual clones within the pool. As the final product, plasmid pDP81 carrying the insert shown in Fig. 1B was isolated, and its origin from *M. smegmatis* was verified by Southern blot hybridization.

RNA isolation. RNA was extracted by the CsCl isolation technique (5, 27). A 100-ml liquid broth was inoculated with 1 ml of saturated *M. smegmatis* culture and grown with vigorous shaking (250 rpm) for 5 h (optical density at 600 nm [OD_{600}] of 0.3). The culture was rapidly cooled on dry ice by intensive swirling to avoid freezing, and bacteria were collected by centrifugation. The pellet was resuspended in 1 ml of ice-cold lysis buffer (50 mM Tris-HCl [pH 7.5]), transferred to 1.5-ml polypropylene vials with neoprene O rings (Biospec Products) containing 700 mg of glass beads (425 to 500 μm; Sigma), and disrupted by beating for 1 min in a Mini Beadbeater-8 (Biospec Products) at maximum speed (2,800 rpm); 200 μl of 20% sodium dodecyl sulfate (SDS) was added to disrupted cells, and the mixture was incubated for 1 min at 67°C. After a brief centrifugation in an Eppendorf centrifuge, the supernatant was transferred to a 13-ml Sarstedt tube, and 10 ml of lysis buffer with dissolved 4 g of CsCl added. The mixture was centrifuged at 11,000 rpm in an SM-24 rotor for 10 min at room temperature. The clarified supernatant was layered on top of a 2-ml 5.7 M CsCl cushion and centrifuged in an SW50.1 rotor for 12 h at 35,000 rpm and 15°C. The translucent RNA pellet was dissolved in H_2O, extracted with chloroform, and pelleted with 2.5 volumes of ethanol. RNA was stored under ethanol and dissolved in H_2O immediately prior to use. The RNA concentration was determined spectrophotometrically.

S1 nuclease protection analysis. S1 nuclease protection analysis was carried out as previously described (5, 27). To generate a uniformly labeled single-stranded DNA probe, a 1.2-kb *Pst*I fragment of the insert in pDP81 was subcloned in the phagemid vector pUC118, resulting in plasmid pDP82. Single-stranded *ahpC* template was prepared by transforming INVα cells (Invitrogen) and superinfecting them with the helper phage M13KO7 according to published protocols (1). Single-stranded ^{32}P-radiolabeled probe was prepared as described previously (5, 27), using the primer AhpS1 (5′GGTGAAGTAGTCATCGGG CTG3′) and *ahpC* template. The polymerization products were digested with *Ava*II and heat denatured in formamide, and the single-stranded probe was gel purified. The probe was annealed to mRNA in a hybridization reaction with 100 μg of total RNA for 1 h at 67°C. Hybridization products were digested for 30 min at 37°C by the addition of 1,200 U of S1 nuclease (Boehringer Mannheim) and 300 μl of buffer containing 280 mM NaCl, 50 mM sodium acetate (pH 4.6), 4.5 mM $ZnSO_4$, and 20 μg of denatured salmon sperm DNA per ml. S1 nuclease digestion products were precipitated with ethanol and analyzed on a sequencing gel alongside a sequencing ladder generated by using *ahpC* template and the primer AhpS1 to permit location of the mRNA 5′ ends.

Exposure of mycobacteria to peroxides, metabolic labeling of proteins, and immunoblot analysis. *M. smegmatis* and *M. aurum* were grown to an OD_{600} of 0.2 and aliquoted into 1-ml portions in propylene vials. H_2O_2, cumene peroxide, or *tert*-butyl peroxide was added when required, followed by the addition of 10 μCi of [^{35}S]methionine and [^{35}S]cysteine (Expre^{35}S^{35}S protein labeling mix; 1,000 Ci/mmol; DuPont NEN). After 1 h at 37°C, the vials were centrifuged and washed once with 20 mM Tris-HCl (pH 7.5). Bacterial pellets were resuspended in 100 μl of 20 mM Tris-HCl (pH 7.5), and upon addition of 20 μl of zirconium beads (0.1- to 0.15-mm diameter; Biospec Products), cells were homogenized in a Mini Beadbeater for 2 min at 2,800 rpm. The beads and cell debris were removed by centrifugation, and the resulting supernatant was mixed with an equal volume of 2× SDS-polyacrylamide gel electrophoresis (PAGE) sample loading buffer and analyzed on SDS–11% polyacrylamide gels. Either the gels were dried and directly used for autoradiography or proteins were first transferred to Immobilon-P membranes (Millipore) by electroblotting, autoradiographed, and subjected to immunodetection. Western blot (immunoblot) analysis was carried out as described previously (7). Rabbit antiserum to DirA (AhpC) of *Corynebacterium diphtheriae* (1:2,000 dilution) was used to probe mycobacterial AhpC. Anti-rabbit immunoglobulin G conjugated to peroxidase (Kirkegaard & Perry Laboratories) diluted to 1:2,000 was used as the secondary antibody. The antibody bound to the membrane was visualized by formation of diaminobenzidine precipitate.

Inhibition of mycobacterial growth by INH. Overnight cultures of *M. smegmatis* carrying the vector pMV206 or p*MsahpC* were diluted with fresh medium to an OD_{600} of 0.2. Thirty microliters from these cultures was inoculated into 3 ml of medium supplemented with serial dilutions of INH. Growth was assessed after 4 days of incubation at 37°C. For *M. aurum*, saturated cultures (OD_{600} of 0.5) were diluted with fresh medium to an OD_{600} of 0.15. Fifty microliters from these cultures was added to 3 ml of fresh medium with INH dilutions. Growth was assessed after 4 days of incubation at 30°C. MIC was as previously defined (8).

Nucleotide sequence accession numbers. The sequences reported here have been deposited in GenBank with the following accession numbers: (i) U31978 for the *M. smegmatis ahpC* structural gene and promoter region; (ii) U43719 for the complete sequence of the 1,701-bp *Bgl*II fragment (Fig. 1B) with regions upstream and downstream of *ahpC*; (iii) U43886 for the *oxyR-ahpC* intergenic region from *M. tuberculosis* B1453; (iv) U43812 for the *oxyR-ahpC* intergenic region from *M. tuberculosis* 24; and (v) U43947 for the *oxyR-ahpC* intergenic region from *M. bovis* ATCC 35747.

RESULTS

Cloning and characterization of the *ahpC* gene from *M. smegmatis* and mapping of its mRNA 5′ ends. To isolate and characterize the putative *ahpC* and *oxyR* homologs from *M. smegmatis*, we used *oxyR* and *ahpC* from several mycobacteria as hybridization probes. *M. tuberculosis ahpC* gave a strong hybridization signal with *M. smegmatis* chromosomal DNA (data not shown). In contrast, under low-stringency conditions, *oxyR* probes from several mycobacterial species produced only very weak signals which did not overlap with the *ahpC* hybridization patterns. The specific hybridization of *M. smegmatis* genomic blots with *ahpC* probes permitted us to clone (see Materials and Methods) and characterize the corresponding region from the *M. smegmatis* chromosome. The nucleotide sequence of the region hybridizing with the *M. tuberculosis* probe (Fig. 2) revealed the presence of a gene encoding a putative polypeptide displaying high-level similarities (38 to 79% identity) with previously characterized bacterial AhpC homologs or functional equivalents (3, 4, 16, 34).

Sequence analysis of the region immediately upstream of *M. smegmatis ahpC* did not indicate any detectable similarities with the conserved features in the region upstream of *ahpC* in several other mycobacteria studied (8, 21, 28, 38). Further-

```
                                                          P1      P2
1   TGTGGAGAATCACGGCTCAGCAAAGTTGCATTTGTAAGAGGGCGCGACCAGAATCGTGGTGTAAATCTGGAATCATTCCAGAAAACAAGAACACGTAGAT

101 GGGATGCTGTGAATGGCTCTTTTGACGATCGGTGACCAGTTTCCGGAGTACGACCTGACCGCTGTGGTTGGCGGCGATCTGTCCAAGGTTGACGCCAAGC
                M  A  L  L  T  I  G  D  Q  F  P  E  Y  D  L  T  A  V  V  G  G  D  L  S  K  V  D  A  K  Q

201 AGCCCGATGACTACTTCACCCGCGTCACCAGCAAGGATTACGAGGGCAAGTGGCGCATCATCTTCTTCTGGCCCAAGGACTTCACGTTCGTGTGCCCGAC
      P  D  D  Y  F  T  R  V  T  S  K  D  Y  E  G  K  W  R  I  I  F  F  W  P  K  D  F  T  F  V  C  P  T

301 GGAGATCGCGGCCTTCGGCAAGCTGAACGAGGACTTCGAGGACCGCGACGCCAAGGTGCTCGGTGTGTCGGTGGACAACGAGTTCGTCCACTTCCAGTGG
      E  I  A  A  F  G  K  L  N  E  D  F  E  D  R  D  A  K  V  L  G  V  S  V  D  N  E  F  V  H  F  Q  W

401 CGTGCACAGCACGAGGACCTCAAGACCCTGCCCTTCCCGATGGTCTCGGATCTCAAGCGTGAGCTGACCGCCGCGTGCGGCGTGCTCAACGCCGACGGTG
      R  A  Q  H  E  D  L  K  T  L  P  F  P  M  V  S  D  L  K  R  E  L  T  A  A  C  G  V  L  N  A  D  G  V

501 TCGCCGACCGCGCGACCTTCATCGTCGACCCCAACAACGAGGTCCAGTTCGTGTCGGTGACCGCGGGCTCGGTGGGCCGCAACGTCGACGAGGTGCTGCG
      A  D  R  A  T  F  I  V  D  P  N  N  E  V  Q  F  V  S  V  T  A  G  S  V  G  R  N  V  D  E  V  L  R

601 CGTGCTCGACGCGCTGCAGTCCGACGAACTGTGCGCGTGCAACTGGAAGAAGGGCGATCCGACGATCAACGCAGGCGAGCTGCTGGCTGGGGCGGTGTGA
      V  L  D  A  L  Q  S  D  E  L  C  A  C  N  W  K  K  G  D  P  T  I  N  A  G  E  L  L  A  G  A  V  *
```

FIG. 2. Nucleotide sequence of *M. smegmatis ahpC*. Bent arrows (P1 and P2), transcriptional start sites of *ahpC*; underlined bases, putative ribosomal binding site. The gene product of *ahpC* shows 38% identity with AhpC from enteric bacteria and 63% identity with *C. diphtheriae* DirA (which is functionally interchangeable with *E. coli* AhpC [33]). *M. smegmatis* AhpC shows 76 to 79% identity with mycobacterial AhpC sequences (*M. tuberculosis* AhpC [8], *Mycobacterium avium* antigen Avi3 [38], and *M. leprae* AhpC [GenBank accession number L01095]) for which multiple sequence alignments have been previously reported (8).

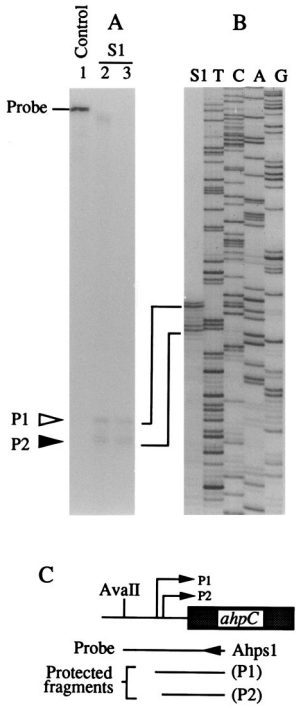

FIG. 3. Mapping of *ahpC* mRNA 5′ ends by S1 nuclease protection analysis. (A) Reduction in size of the uniformly labeled probe upon hybridization with RNA from *M. smegmatis* and S1 nuclease treatment (see Materials and Methods). Lanes: 1, untreated probe; 2 and 3, total *M. smegmatis* RNA from two independently grown cultures. (B) Alignment of the bands of protection (lane S1) with the corresponding *ahpC* sequence (lanes T, C, A, and G). The sequence was generated by using the same oligonucleotide, Ahps1 (see panel C), that was used to obtain uniformly labeled single-stranded probe (see Materials and Methods). (C) Schematic representation of the probe and protected fragments in relationship to *ahpC* and its upstream region. P1 and P2, *ahpC* mRNA start sites.

more, sequence analysis of a region 1 kb upstream of *ahpC* (Fig. 1B; sequence deposited under GenBank accession numbers U31978 and U43719) indicated that, unlike in other mycobacteria studied thus far, no candidate *oxyR* gene could be discerned upstream of *ahpC*. Global similarity searches and other computer analyses did not reveal any significant open reading frames in this region.

To investigate whether the *ahpC* promoter is located further upstream, thus potentially misplacing *oxyR* from its usual location in the vicinity of *ahpC* (e.g., by insertion of another gene between *ahpC* and *oxyR*), we examined transcription in this region and mapped the 5′ ends of *ahpC* mRNA by S1 nuclease protection analysis utilizing previously described approaches (5, 27). The results of these studies (Fig. 3) indicated that there were two mRNA 5′ ends located at positions −48 and −54 relative to the initiation codon of *ahpC*. These studies show that the *ahpC* promoter is located immediately upstream of the structural gene for *ahpC* in *M. smegmatis.*

Differential induction of nine polypeptides in *M. smegmatis* upon exposure to H_2O_2 or organic peroxides. We next investigated whether *M. smegmatis* can induce AhpC in response to challenge with different peroxides. We first examined whether exposure to peroxides can cause differential gene expression in this organism by metabolic labeling of newly synthesized proteins. A distinct induction pattern of de novo protein synthesis with upregulation of several polypeptides was observed upon exposure to H_2O_2 (Fig. 4A). The majority of the polypeptides induced with H_2O_2 were also inducible by two alkyl peroxides tested, cumene hydroperoxide and *tert*-butyl hydroperoxide (Fig. 4A).

Each inducible polypeptide was termed Osp (for oxidative stress *M. smegmatis* protein) followed by a number denoting its apparent M_r (in thousands) as determined from corresponding electrophoretic mobilities on SDS-polyacrylamide gels and a letter denoting inducibility with different agents (H, H_2O_2; A, both alkyl hydroperoxides tested; or C, cumene hydroperoxide). A total of nine peroxide-inducible polypeptides were detected (Fig. 4A and data not shown). Of these, six polypeptides with apparent molecular masses of 17 kDa (Osp17H/A), 19 kDa

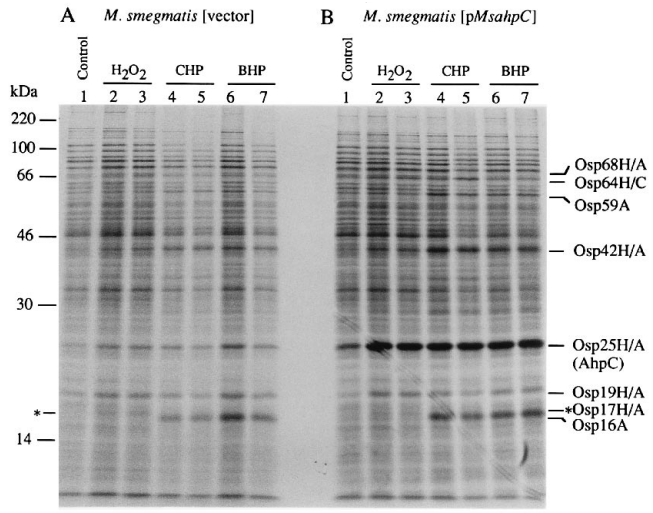

FIG. 4. *M. smegmatis* response to peroxides (A) and indication that the peroxide-inducible polypeptide Osp25H/A is the gene product of *M. smegmatis ahpC* (B). Each lane contained total protein extracts (obtained by bead beating) from 1-ml aliquots of *M. smegmatis* culture grown as described in Materials and Methods, treated with peroxides, labeled with [^{35}S]Met-[^{35}S]Cys for 1 h at 37°C, separated by SDS-PAGE, and analyzed by autoradiography. The only difference between panels A and B is the presence of the plasmid p*MsahpC* in the strain in panel B. CHP, cumene hydroperoxide; BHP, *tert*-butyl hydroperoxide. Lanes: 1, no treatment; 2, 4, and 6, 62.5 μM peroxide (specific compounds indicated above each set); 3, 5, and 7, 125 μM peroxide. See text for designations of induced polypeptides. Note the increased Osp25H/A intensity in extracts from cells with plasmid-borne *ahpC*. Asterisks on both sides of the autoradiogram denote Osp17H/A, which is more clearly visible at higher H_2O_2 concentrations (not shown) and is distinct from Osp16A.

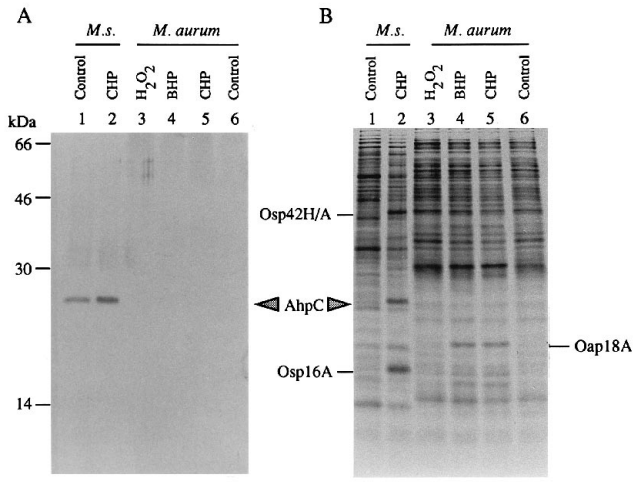

FIG. 5. Immunological detection of AhpC in *M. smegmatis*, using an antibody against *C. diphtheriae* DirA, a functional analog of *E. coli* AhpC (33) (A), and a limited response to peroxide stress in *M. aurum* (B). All samples represent total extracts from 1-ml culture aliquots exposed to peroxides as indicated and metabolically labeled with [^{35}S]Met-[^{35}S]Cys for 1 h at 37°C. The proteins were separated by SDS-PAGE and blotted onto an Immobilon-P membrane. (A) Western blot analysis using antibodies against DirA (AhpC) from *C. diphtheriae*. The secondary antibody was peroxidase-conjugated anti-rabbit immunoglobulin G, and the bands were visualized by incubation with diaminobenzidine and H_2O_2. (B) Autoradiogram of metabolically labeled proteins in panel A before processing for immunodetection. Lanes: 1 and 2, *M. smegmatis* (*M.s.*) untreated (control) and treated with 62.5 μM cumene hydroperoxide (CHP); 3 to 5, *M. aurum* treated with 62.5 μM H_2O_2, *tert*-butyl hydroperoxide (BHP), and cumene hydroperoxide, respectively; 6, untreated *M. aurum*. Note the presence of a single band in panel A corresponding to Osp25H/A in Fig. 4, labeled here as AhpC. (The antibody reacts with the preformed AhpC; hence it is recognized in panel A, lane 1, although AhpC is not discernible by metabolic labeling in the corresponding lane in panel B.) Also note the relative paucity of response (a single prominent band, Oap18A; see text for nomenclature) to peroxide challenge in *M. aurum.*

(Osp19H/A), 25 kDa (Osp25H/A), 42 kDa (Osp42H/A), 64 kDa (Osp64H/C), and 68 kDa (Osp68H/A) responded to H_2O_2 treatment. Another 50-kDa polypeptide, Osp50H, was observed only at H_2O_2 concentrations exceeding 125 μM (data not shown) and was not induced by organic peroxides. Two alkyl peroxide-inducible polypeptides, Osp16A and Osp59A, were inducible with both cumene and *tert*-butyl hydroperoxide (Fig. 4), but no increased synthesis was observed upon exposure to H_2O_2. Osp17H/A showed a clear induction with H_2O_2, but its response to alkyl hydroperoxides depended on other culture conditions and its presence was not always discernible. Collectively, these results indicate that *M. smegmatis* has a significant peroxide stress response.

AhpC is the *M. smegmatis* peroxide-inducible polypeptide Osp25H/A. To determine whether any of the peroxide-inducible polypeptides correspond to AhpC, we introduced plasmid p*MsahpC*, with a 1.7-kb fragment carrying the *M. smegmatis ahpC* gene cloned on a mycobacterial plasmid vector, into *M. smegmatis*. The rationale was that the increased copy number of *ahpC* could result in the increased intensity of the band corresponding to AhpC. The presence of plasmid p*MsahpC* in the cells resulted in increased expression of Osp25H/A and did not affect the induction pattern of other peroxide-inducible polypeptides (Fig. 4B). This result strongly suggested that Osp25H/A could be the gene product of *ahpC*. To confirm this possibility, we used antibodies against a functional AhpC analog from *C. diphtheriae*, DirA (33). DirA is highly similar to *M. smegmatis* AhpC (63% identity) and is functionally interchangeable with AhpC from *E. coli* (33). The DirA-specific antiserum recognized Osp25H/A in *M. smegmatis* (Fig. 5A). This antibody recognized Osp25H/A in both uninduced and induced cells, showing somewhat increased amounts under inducing conditions, as illustrated in Fig. 5A, lanes 1 and 2. These results indicated that the 25-kDa peroxide-inducible polypeptide is the gene product of *M. smegmatis ahpC*. The slightly higher apparent molecular mass of *M. smegmatis* AhpC compared with that predicted from its sequence, 21,624 Da, can be attributed to the low pI of AhpC (4.26), which, as has been previously shown for highly acidic proteins, frequently results in anomalous electrophoretic mobility.

Plasmid-borne *ahpC* reduces inhibitory effects of INH in *M. smegmatis*. To address the possibility that AhpC expression levels affect mycobacterial sensitivity to INH, we examined whether introduction of plasmid-borne *ahpC* could alter the

TABLE 2. Plasmid-borne *ahpC* increases the MIC of INH in *M. smegmatis*

Strain	Plasmid or relevant property	MIC for INH (μg/ml)[a]
M. smegmatis mc^{2}155	pMV206 (vector)	20
	p*MsahpC*	40
M. bovis BCG ATCC 35735		<0.25
M. bovis BCG ATCC 35747	INH^r derivative of ATCC 35735	>50
M. aurum ATCC 23366		<0.625
M. tuberculosis H37Rv		<0.25

[a] Determined as previously described (8). The values for *M. bovis*, *M. tuberculosis*, and *M. aurum* are shown for comparison purposes; similar MICs for the organisms from the *M. tuberculosis* complex have been previously reported.

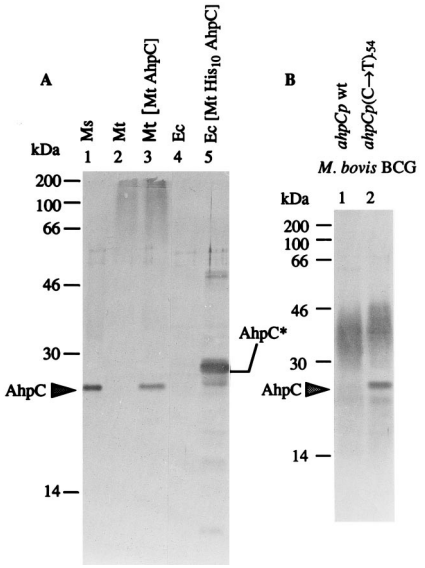

FIG. 6. Analysis of *ahpC* expression in *M. tuberculosis* (A) and detection of AhpC in *M. bovis* BCG carrying a mutation in the *ahpC* promoter region (B). Crude extracts from *M. smegmatis* (Ms), *M. tuberculosis* H37Rv (Mt), *E. coli* (Ec), or *M. bovis* BCG were separated by SDS-PAGE and subjected to Western blot analysis with an antibody against *C. diphtheriae* DirA (AhpC) as for Fig. 5. (A) Lanes, 1, *M. smegmatis*; 2 and 3, *M. tuberculosis* harboring the vector pSMT3 (*oriM oriE* Hyg^r) or plasmid p*MtahpC* with *M. tuberculosis ahpC* on a 5.5-kb *Bam*HI fragment cloned in pSMT3; 4, *E. coli* harboring the T7 expression vector pET-16b; 5, *E. coli* harboring the expression construct p*Mthis$_{10}$-ahpC* with an in-frame fusion between the His_{10} tag and the coding sequence of *ahpC* (see Materials and Methods) (transcription from the T7 promoter was induced in lane 5 by the addition of 1 mM isopropylthiogalactopyranoside (IPTG). Note the absence of AhpC (below the detection level) in *M. tuberculosis* (lane 2) and the ability to detect *M. tuberculosis* AhpC when a plasmid-borne *ahpC* was present in *M. tuberculosis* H37Rv (lane 3) or upon expression from T7 promoter in *E. coli* (lane 5). The increased electrophoretic mobility of the product (AhpC*) detected in *E. coli* is due to the fusion between the His_{10} tag encoded by the expression vector and the entire *M. tuberculosis* AhpC. (B) Lanes: 1, *M. bovis* BCG Montreal (ATCC 35735) with the wild-type *ahpC* promoter (*ahpCp* wt); 2, its derivative ATCC 35747 with a mutation ($C \rightarrow T_{-54}$) in the *oxyR-ahpC* intergenic region 54 bp upstream of the *ahpC* start codon (see Fig. 7).

FIG. 7. Nucleotide substitutions in the intergenic region between *oxyR* and *ahpC* in *M. tuberculosis* strains with deletions in *katG*. Shown is the *M. tuberculosis* H37Rv intergenic region sequence. Triangles, alterations observed in Δ*katG* strains relative to H37Rv or *M. bovis* BCG: G-to-A transition at −88 and T-to-A transition at −76 in *M. tuberculosis* B1453; C-to-T transition at −54 in *M. tuberculosis* 24 and *M. bovis* ATCC 35747. Numbering is given relative to the initiation codon of *ahpC*, and variant nucleotides are shown in boldface. Divergent arrows, the 5′ ends of *ahpC* and *oxyR* genes (*oxyR* is inactivated by multiple mutations [Fig. 1]). Boxes: three nucleotides, *ahpC* initiation codon; four nucleotides, predicted mutation (#) destroying the *oxyR* initiation codon in all strains of *M. tuberculosis* (8).

level of *M. smegmatis* sensitivity to INH. *M. smegmatis ahpC*, cloned as a 1.7-kb *Bgl*II fragment (Fig. 1B), was introduced into *M. smegmatis* mc^{2}155, in which it was shown to increase the basal level of AhpC production (Fig. 4B). The results displayed in Table 2 indicated that the presence of plasmid-borne *ahpC* increased the MIC of INH relative to that for the control strain harboring the vector only. Inhibition with other antibiotics was not affected (data not shown). The modest effect in *M. smegmatis*, relative to the previously published increase in MIC of INH (from 0.05 to 5 μg/ml) in *M. tuberculosis* H37Rv harboring a functional *oxyR-ahpC* clone from *M. leprae* (8), can be at least partially attributed to the high intrinsic level of INH resistance in *M. smegmatis*. Nevertheless, it is possible to conclude that additional copies of *ahpC* present in *M. smegmatis* reduced its sensitivity to the inhibitory action of INH.

Absence of detectable AhpC in *M. tuberculosis* and *M. aurum*, mycobacterial species highly sensitive to INH. The exquisite INH sensitivity of *M. tuberculosis* relative to other mycobacteria has been linked to the multiple lesions in *oxyR* of this organism (8). One consequence of *oxyR* inactivation in *M. tuberculosis* could be a negative effect on AhpC expression. To investigate this possibility, we first examined whether AhpC could be detected in *M. tuberculosis* extracts by using the antibody used to detect the *M. smegmatis ahpC* gene product. *M. tuberculosis* H37Rv did not show detectable AhpC (Fig. 6A, lane 2). However, when *M. tuberculosis ahpC* was cloned on a mycobacterium-*E. coli* shuttle vector and *M. tuberculosis* H37Rv was transformed with the resulting plasmid, AhpC was clearly detectable in this organism (Fig. 6A, lane 3). To independently confirm that the antibody against *C. diphtheriae* DirA recognized in these experiments the *M. tuberculosis ahpC* gene product, *M. tuberculosis ahpC* was fused to an oligo-His tag and cloned in a T7 expression vector, and a hybrid polypeptide (His_{10}-AhpC) was overproduced and detected in *E. coli* (Fig. 6A, lane 5). These experiments demonstrated that the antibody recognizing *M. smegmatis* AhpC reacted with *M. tuberculosis* AhpC and indicated that the basal level of AhpC expression in *M. tuberculosis* was too low to permit its detection. These findings support the interpretation that *ahpC* expression in *M. tuberculosis* is lower than in organisms such as *M. smegmatis.*

Another mycobacterium known to be naturally highly sensitive to INH is *M. aurum*. To initiate studies aimed at investigating whether the INH sensitivity of this organism is related to the observed phenomena in *M. tuberculosis*, we analyzed *M. aurum* ATCC 23366. The MIC of INH for this species type strain was 0.625 μg/ml (Table 2). Similar INH sensitivities have been observed by others (17a). We tested *M. aurum* for the presence of detectable AhpC by using the same antibody shown to react with *M. smegmatis* and *M. tuberculosis* AhpC. The results of these experiments indicated that *M. aurum* had no immunologically detectable AhpC under conditions identical to those used for *M. smegmatis* (Fig. 5A). No polypeptide reactive with the anti-DirA antibody could be detected in extracts from *M. aurum* grown under standard conditions or upon exposure to H_2O_2 and organic peroxides which induced AhpC synthesis in *M. smegmatis*. Moreover, by examining patterns of metabolically labeled proteins, no significant peroxide-inducible polypeptides in the M_r range corresponding to a typical AhpC could be observed (Fig. 5B). Only one polypeptide with an apparent molecular mass of 18 kDa was differentially induced by peroxide stress in *M. aurum* (Oap18A, for oxidative stress *M. aurum* protein). The de novo synthesis of Oap18A was stimulated by organic peroxides but not by H_2O_2 (Fig. 5B), reminiscent of the induction pattern seen with Osp16A in *M. smegmatis*. In a complementary set of experiments, hybridization studies using the known *ahpC* genes as probes which hybridized with all other mycobacteria tested failed to produce a specific signal in *M. aurum* ATCC 23366,

congruent with the results of metabolic labeling and Western blot analyses.

Mutations in the intergenic *oxyR-ahpC* region in INH^r *M. tuberculosis* strains with deletions in *katG*. A proposed role of *ahpC* in reducing susceptibility to INH (8, 23) and its well-documented role in detoxifying products of endogenously generated reactive oxygen intermediates in enteric bacteria (4, 10, 16) prompted us to evaluate the regulatory region between *ahpC* and *oxyR* in INH^r strains of *M. tuberculosis*. In this work, we report the surprising finding that the previously characterized (41) Δ*katG* clinical strains of *M. tuberculosis*, B1453 and 24, displaying high-level INH resistance, as well as an INH^r derivative of *M. bovis* BCG Montreal (ATCC 35747) which has a 507-bp deletion removing the N-terminal portion of *katG* (25), also carry mutations or polymorphisms in the 105-bp intergenic region between *oxyR* and *ahpC* (Fig. 7). Significantly, the Δ*katG* BCG strain examined carried a mutation identical to the variant nucleotide present in the strain 24 at position −54 relative to the start codon of *ahpC*. Western blot analyses indicated that *ahpC* expression was higher in strain ATCC 35747 than in the parental strain *M. bovis* BCG Montreal (Fig. 6B). These data suggest that Δ*katG* strains of the *M. tuberculosis* complex frequently (in all three Δ*katG* isolates tested) contain additional mutations, such as those described here, which could contribute to their overall level of sensitivity to INH. Alternatively or in addition, mutations enhancing *ahpC* expression may compensate for the lack of catalase in Δ*katG* strains, which could impose an additional burden on detoxification of endogenously generated reactive oxygen species.

DISCUSSION

The results reported in this study support a correlation between the defect in oxidative stress response and high sensitivity to INH of some mycobacteria. The reported studies also expand the intriguing peculiarities concerning the regulators and control of oxidative stress response in mycobacteria (8, 12, 28) and provide new insights into the basic biology of these organisms. For example, the absence of *oxyR* in the region upstream of *M. smegmatis ahpC* contrasts with the previously described arrangement considered to be typical for mycobacteria as epitomized by the tightly linked and divergently transcribed *oxyR* and *ahpC* genes in *M. leprae* and several other mycobacterial species (8, 21, 28). Since sequence analysis of the 953-bp region upstream of *ahpC* in *M. smegmatis* ruled out a presence of *oxyR*-like sequences in this region, it is reasonable to conclude that *M. smegmatis* differs in genetic organization from the mycobacteria studied thus far. However, the inducibility of AhpC along with eight other polypeptides strongly suggests the existence of a peroxide response regulator in this organism. Further analyses are needed to determine whether and to what extent the putative regulatory elements of peroxide stress response in *M. smegmatis* may resemble the *M. leprae*/*M. tuberculosis* paradigm (Fig. 1).

Interestingly, *C. diphtheriae dirA*, a functional analog of *ahpC* (33), has no significant open reading frames within the investigated region extending 600 bp upstream of the *dirA* structural gene, which is reminiscent of the situation with *M. smegmatis ahpC*. It is also worth mentioning that immediately downstream of *dirA* in *C. diphtheriae* there is an open reading frame with the capacity to code for a 19-kDa polypeptide (33). In *M. tuberculosis* (GenBank accession number U44840), *M. bovis* (GenBank accession number U24083), and *M. leprae* (GenBank accession number L01095; with several sequence corrections [our unpublished analysis]), there is an open reading frame downstream of *ahpC* with the capacity to code for an 18- to 19-kDa polypeptide. This putative polypeptide shows strong conservation with the predicted product of a gene downstream of *M. smegmatis ahpC* (data not shown). In *E. coli* and *Salmonella typhimurium*, alkyl hydroperoxide reductase consists of two separable components (21), AhpC and AhpF. The *ahpC* and *ahpF* genes are tightly linked and coordinately inducible by H_2O_2 (10, 32). While AhpC directly reduces organic peroxide substrates and is highly homologous to mycobacterial AhpC and *Corynebacterium* DirA, AhpF (a 57-kDa flavoprotein) reduces AhpC by using NAD(P)H as the electron donor (16). Although the conservation of *ahpC* and the downstream gene in mycobacteria suggests a relationship potentially similar to that for the two components of alkyl hydroperoxide reductase in enteric organisms (16, 32), any such relationships and enzymatic activities remain to be biochemically investigated before conclusions can be made. Future enzymatic studies with the gene product of mycobacterial *ahpC* and the putative downstream components may help define physiological substrates of relevance for mycobacterial physiology that could potentially explain the apparent role of AhpC in counteracting the action of INH in these organisms.

From what is known about AhpC in enteric organisms (11, 16, 31), the mycobacterial equivalent could also participate in conversion of physiologically relevant and potentially harmful or mutagenic hydroperoxide derivatives of lipids and nucleic acids into corresponding alcohols. It has been proposed that INH taken up by mycobacterial cells undergoes peroxidatic activation into its active form in a reaction dependent on catalase-peroxidase (39, 42). In addition, it has been shown that INH can stimulate production of reactive oxygen intermediates in the presence of H_2O_2 and transition metals or peroxidase (17, 29, 36). Since AhpC has been implicated in detoxification and reduction of various exogenously supplied or endogenously generated organic hydroperoxides (4, 16), this enzyme may play a role by directly reducing toxic INH products or ameliorating possible consequences of increased oxidative damage to cell molecules. In indirect but important support of such notions are the observations by Rosner (23) and Rosner and Storz (24) that *E. coli* can be rendered sensitive to INH by inactivation of its *ahpC*.

Perhaps the most relevant finding presented here is the observation regarding the dramatic differences in the levels of AhpC in *M. smegmatis* and *M. tuberculosis*. These observations are in keeping with the results of *ahpC* transcriptional fusion studies suggesting that *M. tuberculosis ahpC* is transcribed at lower levels than *M. leprae ahpC* (9). In variance with our findings, Sherman and colleagues (28) presented RNA slot blot hybridization data obtained with a heterologous probe which suggest a higher level of basal expression of *ahpC* in *M. tuberculosis* than in *M. smegmatis*. Additional RNA studies using specific autologous probes and techniques less prone to errors (e.g., S1 nuclease protection analysis) will be needed to assess more precisely the transcription of *ahpC* in *M. tuberculosis*. Such studies along with those that remain to be performed with *M. smegmatis* under inducing conditions should help refine our understanding of the relative responsiveness of *ahpC* to oxidative stress challenge in each mycobacterium studied. The mapping of the two 5′ ends of *M. smegmatis ahpC* presented here and the ongoing studies defining promoter elements within the *oxyR-ahpC* intergenic region in *M. tuberculosis* will facilitate such analyses and are expected to help delimit *cis*-acting regulatory elements controlling expression of the *ahpC* and *oxyR* genes.

The higher levels of AhpC in *M. smegmatis* than in *M. tuberculosis* are in keeping with the model proposing *ahpC* ex-

pression defect in *M. tuberculosis*, a phenomenon that can be at least partially attributed to the *oxyR* lesions in the tubercle bacillus (8). The inactivation of *oxyR* has already been linked to the naturally high INH sensitivity of *M. tuberculosis* (8), and the studies presented here provide further support of this model. Similar to the observations with *M. tuberculosis*, we could not detect AhpC in another INH-sensitive organism, *M. aurum*. The potential relationship of the apparent lack of AhpC or its expression with the high natural sensitivity of *M. aurum* to INH and the genetic basis for these phenomena remain to be further investigated but nevertheless appear to be congruent with the concepts discussed above.

In an earlier report, plasmid-borne *M. leprae oxyR-ahpC* increased the MIC of INH in *M. tuberculosis* to 5 μg/ml (8). In repeated experiments with *M. tuberculosis* H37Rv transformed with autologous *M. tuberculosis ahpC*, interpretation of INH inhibition results was complicated by the emergence of catalase-negative mutants displaying resistance to INH concentrations as high as 50 μg/ml. Nevertheless, the observations reported here concerning the absence of detectable AhpC in *M. tuberculosis* and *M. aurum* along with the effects of the introduction of extra copies of *ahpC* into *M. smegmatis*, which further augment its natural resistance to INH, and the previously reported complementation experiments in *M. tuberculosis* (8) are consistent with the interpretation that *ahpC* expression and INH sensitivity are inversely related in mycobacteria. Furthermore, we have recently inactivated *ahpC* on the chromosome of *M. smegmatis* and observed increased sensitivity to INH of the mutant strain relative to its $ahpC^+$ parent (40).

An intriguing finding of point mutations within the *M. tuberculosis oxyR-ahpC* intergenic region in strains highly resistant to INH suggests a possible relationship to the emergence of INH^r strains. In one model that is currently being considered, it is possible that mutations increasing *ahpC* expression play a direct role in INH resistance. However, the apparently high incidence (in three strains presented here and in four additionally tested strains; GenBank accession numbers U57760, U57761, U57762, and U58031 [40]) of such alterations in INH^r isolates with completely inactivated *katG* (25, 41) suggests that these changes may be selected as compensatory mutations. For example, elevated AhpC levels could enhance protection against unchecked endogenous H_2O_2 levels in cells devoid of catalase, since disproportionation of this harmful pro-oxidant is no longer possible via the gene product of *katG*. Future analyses will help distinguish between these two possibilities and provide an estimate of the relative contributions of such mutations to the emergence of high-level resistance to INH in clinical *M. tuberculosis* isolates, as well as their frequency in INH^r strains which do not carry *katG* mutations.

It is becoming increasingly evident not only that INH is a clinically superior antituberculosis agent but also that it has been instrumental in the uncovering of a surprising weakness of *M. tuberculosis*, namely, that this organism is a mutant in *oxyR* (8). These lesions most likely underlie the observations that *M. tuberculosis* is unable to mount a significant peroxide stress response (8, 12) although it can respond to other challenges (e.g., the recently defined nitric oxide response [12]). In contrast, *M. smegmatis* shows a peroxide induction pattern of at least nine distinct Osp polypeptides as reported in this work. Future analyses of the functions of these proteins and characterization of the corresponding genes in this organism may help elucidate their physiological and possibly protective roles and could provide a means to study elements of the peroxide stress response systems that may exist but are not expressed at adequate or adjustable levels in *M. tuberculosis*. Such comparative studies in model mycobacterial organisms will help lead to an understanding of the repercussions of the *oxyR* defect in *M. tuberculosis* on the physiology of this bacterium, with possible significance for improved or novel drug design based on peroxide stress response deficiency. These studies, while anticipated to be of high practical value, will also continue to provide insights into fascinating fundamental biological aspects of the formidable human pathogen *M. tuberculosis.*

ACKNOWLEDGMENTS

We thank S. S. Tai for the gift of the anti-DirA antibody; I. Orme and D. B. Young for *M. tuberculosis* B1453 and 24; T. Garbe for contributing to the analysis of *ahpC* in *M. tuberculosis*; C. Lacave for clarifying previously published information on *M. aurum* sensitivity to INH; and H. Yu for constructive criticisms of the manuscript.

This work was supported by grant AI35217 from the National Institute of Allergy and Infectious Diseases.

REFERENCES

1. **Ausubel, F. M., R. Brent, R. E. Kingston, D. D. Moore, J. G. Seidman, J. A. Smith, and K. Struhl (ed.).** 1989. Current protocols in molecular biology. John Wiley & Sons, New York.
2. **Banerjee, A., E. Dubnau, A. Quemard, V. Balasubramanian, K. S. Um, T. Wilson, D. Collins, G. de Lisle, and W. R. Jacobs, Jr.** 1994. *inhA*, a gene encoding a target for isoniazid and ethionamide in *Mycobacterium tuberculosis*. Science **263:**227–230.
3. **Chae, H. Z., K. Robison, L. B. Poole, G. Church, G. Storz, and S. G. Rhee.** 1994. Cloning and sequencing of thiol-specific antioxidant from mammalian brain: alkyl hydroperoxide reductase and thiol-specific antioxidant define a large family of antioxidant enzymes. Proc. Natl. Acad. Sci. USA **91:**7017–7021.
4. **Christman, M. F., R. W. Morgan, F. S. Jacobson, and B. N. Ames.** 1985. Positive control of a regulon for defenses against oxidative stress and some heat-shock proteins in *Salmonella typhimurium*. Cell **41:**753–762.
5. **Curcic, R., S. Dhandayuthapani, and V. Deretic.** 1994. Gene expression in mycobacteria: transcriptional fusions based on *xylE* and analysis of the promoter region of the response regulator *mtrA* from *Mycobacterium tuberculosis*. Mol. Microbiol. **13:**1057–1064.
6. **Dannenberg, A. M., Jr., and G. A. W. Rook.** 1994. Pathogenesis of pulmonary tuberculosis: an interplay of tissue-damaging and macrophage-activating immune responses—dual mechanisms that control bacillary multiplication, p. 459–483. *In* B. R. Bloom (ed.), Tuberculosis: pathogenesis, protection, and control. ASM Press, Washington, D.C.
7. **Deretic, V., N. S. Hibler, and S. C. Holt.** 1992. Immunochemical analysis of AlgP(Hp1), a histonelike element participating in control of mucoidy in *Pseudomonas aeruginosa*. J. Bacteriol. **174:**824–831.
8. **Deretic, V., W. Philipp, S. Dhandayuthapani, M. H. Mudd, R. Curcic, T. Garbe, B. Heym, L. E. Via, and S. T. Cole.** 1995. *Mycobacterium tuberculosis* is a natural mutant with an inactivated oxidative-stress regulatory gene: implications for sensitivity to isoniazid. Mol. Microbiol. **17:**889–900.
9. **Dhandayuthapani, S. L. E. Via, C. A. Thomas, P. M. Horowitz, D. Deretic, and V. Deretic.** 1995. Green fluorescent protein as a marker for gene expression and cell biology of mycobacterial with macrophages. Mol. Microbiol. **17:**901–912.
10. **Farr, S. B., and T. Kogoma.** 1991. Oxidative stress responses in *Escherichia coli* and *Salmonella typhimurium*. Microbiol. Rev. **55:**561–585.
11. **Ferrante, A. A., J. Augliera, K. Lewis, and A. M. Klibanov.** 1995. Cloning of an organic solvent-resistance gene in *Escherichia coli*: the unexpected role of alkylhydroperoxide reductase. Proc. Natl. Acad. Sci. USA **92:**7617–7621.
12. **Garbe, T., N. S. Hibler, and V. Deretic.** 1996. Response of *Mycobacterium tuberculosis* to reactive oxygen and nitrogen intermediates. Mol. Med. **2:**134–142.
13. **Heym, B., P. M. Alzari, N. Honore, and S. T. Cole.** 1995. Missense mutations in the catalase-peroxidase gene, *katG*, are associated with isoniazid resistance in *Mycobacterium tuberculosis*. Mol. Microbiol. **15:**235–245.
14. **Heym, B., and S. T. Cole.** 1992. Isolation and characterization of isoniazid-resistant mutants of *Mycobacterium smegmatis* and *M. aurum*. Res. Microbiol. **143:**721–730.
15. **Jacobs, W. R., Jr., G. V. Kalpana, J. D. Cirrilo, L. Pascopella, S. B. Snapper, R. A. Udani, W. Jones, R. G. Barletta, and B. R. Bloom.** 1991. Genetic systems for mycobacteria. Methods Enzymol. **204:**537–555.
16. **Jacobson, F. S., R. W. Morgan, M. F. Christman, and B. N. Ames.** 1989. An alkyl hydroperoxide reductase from *Salmonella typhimurium* involved in the defense of DNA against oxidative damage. J. Biol. Chem. **264:**1488–1496.
17. **Kruger-Thiemer, E.** 1958. Isonicotinic acid hypothesis of the antituberculous action of isoniazid. Am. Rev. Tuberc. **78:**364–367.

17a. **Lacave, C.** Personal communication.
18. **Lirzin, M. L., J. N. Vivien, A. Lepeuple, R. Thibier, and C. Pretet.** 1971. Rapid microbiological estimation of serum isoniazid. Rev. Tuberc. Pneumol. **35:**350–356.
19. **Loewen, P. C., B. L. Trigs, C. S. Geroge, and B. Hrabarchuk.** 1985. Genetic mapping of *katG*, a locus that affects synthesis of the bifunctional catalase-peroxidase hydroperoxidase I in *Escherichia coli*. J. Bacteriol. **162:**661–667.
20. **Middlebrook, G.** 1954. Isoniazid-resistance and catalase activity of tubercle bacilli. Am. Rev. Tuberc. **69:**471–472.
21. **Mudd, M., Y. Zhang, S. Dhandayuthapani, and V. Deretic.** Unpublished results.
22. **Musser, J. M.** 1995. Antimicrobial agent resistance in mycobacteria: molecular genetic insights. Clin. Microbiol. Rev. **8:**496–514.
23. **Rosner, J. L.** 1993. Susceptibilities of *oxyR* regulon mutants of *Escherichia coli* and *Salmonella typhimurium* to isoniazid. Antimicrob. Agents Chemother. **37:**2251–2253.
24. **Rosner, J. L., and G. Storz.** 1994. Effects of peroxides on susceptibilities of *Escherichia coli* and *Mycobacterium smegmatis* to isoniazid. Antimicrob. Agents Chemother. **38:**1829–1833.
25. **Rouse, D. A., and S. L. Morris.** 1995. Molecular mechanisms of isoniazid resistance in *Mycobacterium tuberculosis* and *Mycobacterium bovis*. Infect. Immun. **63:**1427–1433.
26. **Schell, M. A.** 1993. Molecular biology of the LysR family of transcriptional regulators. Annu. Rev. Microbiol. **47:**597–626.
27. **Schurr, M. J., H. Yu, J. C. Boucher, N. S. Hibler, and V. Deretic.** 1995. Multiple promoters and induction by heat shock of the gene encoding the alternative sigma factor AlgU (σ^E) which controls mucoidy in cystic fibrosis isolates of *Pseudomonas aeruginosa*. J. Bacteriol. **177:**5670–5679.
28. **Sherman, D. R., P. J. Sabo, M. J. Hickey, T. M. Arain, G. G. Maharias, Y. Yuan, C. E. Barry III, and C. K. Stover.** 1995. Disparate responses to oxidative stress in saprophytic and pathogenic mycobacteria. Proc. Natl. Acad. Sci. USA **92:**6625–6629.
29. **Shoeb, H. A., B. U. Bowman, Jr., A. C. Ottolenghi, and A. J. Merola.** 1985. Evidence for the generation of active oxygen by isoniazid treatment of extracts of *Mycobacterium tuberculosis* H37Ra. Antimicrob. Agents Chemother. **27:**404–407.
30. **Snapper, S. B., R. E. Melton, S. Mustafa, T. Kieser, and W. R. Jacobs.** 1990. Isolation and characterization of efficient plasmid transformation mutants of *Mycobacterium smegmatis*. Mol. Microbiol. **4:**1911–1919.
31. **Storz, G., M. F. Christman, H. Sies, and B. N. Ames.** 1987. Spontaneous mutagenesis and oxidative damage to DNA in *Salmonella typhimurium*. Proc. Natl. Acad. Sci. USA **84:**8917–8921.
32. **Storz, G., F. J. Jacobson, L. A. Tartaglia, R. W. Morgan, L. A. Silveira, and B. N. Ames.** 1989. An alkyl hydroperoxide reductase induced by oxidative stress in *Salmonella typhimurium* and *Escherichia coli*: genetic characterization and cloning of *ahp*. J. Bacteriol. **171:**2049–2055.
33. **Tai, S. S., and Y. Y. Zhu.** 1995. Cloning of a *Corynebacterium diphtheriae* iron-repressible gene that shares sequence homology with the AhpC subunit of alkyl hydroperoxide reductase of *Salmonella typhimurium*. J. Bacteriol. **177:**3512–3517.
34. **Tartaglia, L. A., G. Storz, M. H. Brodsky, A. Lai, and B. N. Ames.** 1990. Alkyl hydroperoxide reductase from *Salmonella typhimurium*. Sequence and homology to thioredoxin reductase and other flavoprotein disulfide oxidoreductases. J. Biol. Chem. **265:**10535–10540.
35. **Toledano, M. B., I. Kullik, F. Trinh, P. T. Baird, T. D. Schneider, and G. Storz.** 1994. Redox-dependent shift of OxyR-DNA contacts along an extended DNA-binding site: a mechanism for differential promoter selection. Cell **78:**897–909.
36. **Winder, F.** 1959. Catalase and peroxidase in mycobacteria. Am. Rev. Respir. Dis. **81:**68–78.
37. **Winder, F. G.** 1982. Mode of action of the antimycobacteral agents and associated aspects of the molecular biology of the mycobacteria, p. 351–438. *In* C. Ratledge and J. L. Stanford (ed.), The biology of the mycobacteria, vol. 1. Academic Press, London.
38. **Yamaguchi, R., K. Matsuo, A. Yamazaki, M. Takahashi, Y. Fukusawa, M. Wada, and C. Abe.** 1992. Cloning and expression of the gene for the Avi-3 antigen of *Mycobacterium avium* and mapping of its epitopes. Infect. Immun. **60:**1210–1216.
39. **Youatt, J.** 1969. A review of the action of isoniazid. Am. Rev. Respir. Dis. **99:**729–749.
40. **Zhang, Y., S. Dhandayuthapani, and V. Deretic.** Unpublished results.
41. **Zhang, Y., B. Heym, B. Allen, D. Young, and S. Cole.** 1992. The catalase-peroxidase gene and isoniazid resistance of *Mycobacterium tuberculosis*. Nature (London) **358:**591–593.
42. **Zhang, Y., and D. B. Young.** 1993. Molecular mechanisms of isoniazid: a drug at the front line of tuberculosis control. Trends Microbiol. **1:**109–113.